

# An Adaptive Cruise Control System for Autonomous Vehicles

Man Hyung Lee<sup>1</sup>, Hyung Gyu Park<sup>1</sup>, Seok Hee Lee<sup>1,#</sup>, Kang Sup Yoon<sup>2</sup>, and Kil Soo Lee<sup>1</sup>

<sup>1</sup> Graduate School of Mechanical Engineering, Pusan National University, Busan, Korea, 609-735

<sup>2</sup> School of Automotive, Industrial and Mechanical Engineering, Daegu University, Daegu, Korea, 712-714

# Corresponding Author / E-mail: sehlee@pusan.ac.kr, TEL: +82-51-510-2327, FAX: +82-51-514-0685

KEYWORDS: Adaptive Cruise Control System, Autonomus Vehicle, Laser Scanner, APS, CARSIM, SIMULINK

*An adaptive cruise control system with a longitudinal controller that follows a preceding vehicle in autonomous vehicles is proposed. The adaptive cruise control system in a test vehicle recognizes a preceding vehicle located in front of the test vehicle and drives the test vehicle with a safety distance to the preceding vehicle by controlling its accelerator and brake. Vehicle distance errors caused by preceding vehicle distances can be determined by the distance information obtained from the laser scanner installed on the front side of a succeeding vehicle. The acceleration control in a succeeding vehicle performs velocity control by transmitting APS (Acceleration Position Sensor) signals, which can be generated at the speed control unit artificially, to ECU (Electronic Control Unit). An adaptive cruise control system presented in this research is simulated with CARSIM and SIMULINK and its performance is also proved to be very practical after several experimental test on a real car.*

Manuscript received: August 29, 2012 / Accepted: November 22, 2012

## 1. Introduction

In recent years, studies on advanced safety vehicles have been widely conducted.<sup>1-10</sup> Here, safety technologies are divided into two different categories. One is the passive safety that is the concept of manual type safety that includes safety belts installed since the 1950s and protects and minimizes passengers' lives and damages by constraining passenger behaviors after a car accident, and the other is the active safety that is a concept of increasing the driving performance in vehicles under different driving conditions in addition to the easiness of driving based on various electronic control systems. In the active safety technology, the system that maintains a specific velocity without applying the acceleration pedal in order to provide the easiness of driving for long distances is called a cruise control system. In the cruise control driving that represents a constant velocity, the driving is performed through velocity control only. Thus, it is not possible to guarantee the safety from vehicles and obstacles in front of one's vehicle. Therefore, several researches on an adaptive cruise control (ACC) system for monitoring traffic conditions ahead and preventing accidents caused by carelessness have been largely conducted.

In the ACC system, the first thing to considered is the safety of the drivers of the vehicles or obstacles during driving. Thus, the ACC system is divided into two different issues; one is performing longitudinal

control for maintaining a vehicle distance between vehicles and implementing velocity tracking, and the other is lateral control for keeping lanes and preventing lane departure.

In this research, a study of an ACC system for controlling a vehicle according to distance of the preceding vehicle is implemented.<sup>11</sup> A vehicle used to develop the ACC system was an SUV, Mohave manufactured by Kia Motors, and the vehicle was modified. Also, a laser scanner, LMS-291 by SICK, was used to measure the distance in collision and avoidance of the vehicle ahead. A PID controller was designed using a switching logic in order to implement the acceleration and deceleration control of the vehicle. The vehicle distance errors calculated using the stop distance and measured vehicle distance were applied to the input of the PID controller. An acceleration system performs acceleration control using electronic control unit (ECU) based on the signal of APS, which is installed on the vehicle, according to the vehicle distance errors. Also, a deceleration system performs deceleration control based on motor control through connecting an RC servo motor to the brake pedal.

## 2. Hardware Composition

In this section, the characteristics and structures of the vehicle and equipments used to implement the ACC system are described.



Fig. 1 Autonomous vehicle, Kia Mohavi

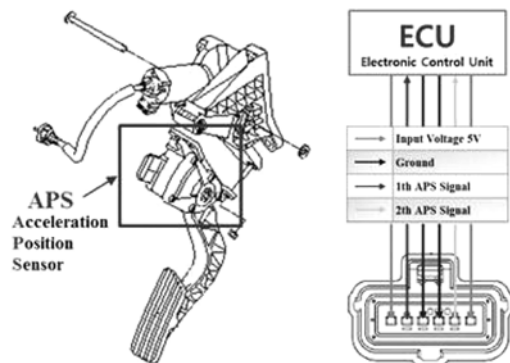


Fig. 2 APS Assembly and APS Pin Arrangement

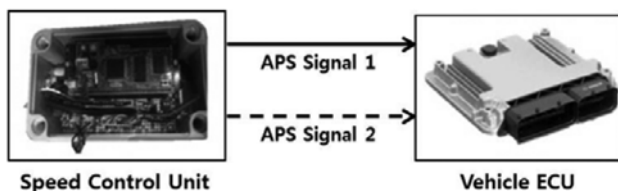


Fig. 3 Acceleration control in vehicle

## 2.1 Autonomous vehicle

The vehicle used in this research was an SUV, Mohave by Kia Motors, with a 3,000cc diesel engine and an automatic transmission. Fig. 1 shows the modified vehicle applied in the experiment of this research. Here, a laser scanner was installed inside the bumper.

## 2.2 Acceleration control system

In preceding studies, a method that controls an actuator directly connected to the throttle body or pedal was used to implement acceleration control.<sup>12</sup> However, in the case of the test vehicle, Mohave, it performs such acceleration control using an acceleration position sensor (APS) installed on the acceleration pedal. Thus, in this research it is proposed that the acceleration control is to be implemented using the APS installed on the test vehicle. The APS includes two independent signals in which these two signals transmit output voltages to ECU through a variable resistor installed on the acceleration pedal in order to perform acceleration control of the vehicle. Fig. 2 shows the installed configuration of the APS.

Fig. 3 represents the method proposed in this research. Table 1

Table 1 APS specification

| State             | Output Voltage (V) |               |
|-------------------|--------------------|---------------|
|                   | APS 1              | APS 2         |
| Idle State        | 0.7 ~ 0.8          | 0.275 ~ 0.475 |
| Full Acceleration | 3.8 ~ 4.4          | 1.75 ~ 2.35   |

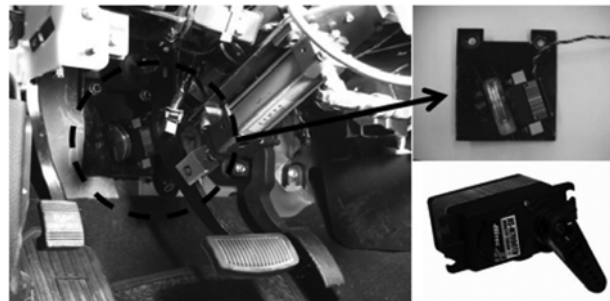


Fig. 4 Servo motor is equipped on the brake pedal

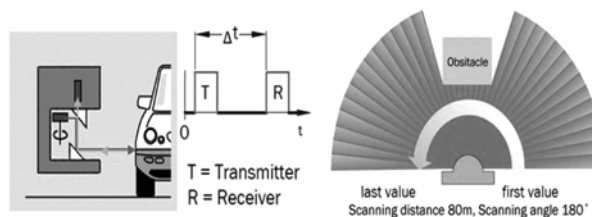


Fig. 5 Operating principles and angular range of laser scanner

shows the results of the analysis of the output signals from the APS installed on this test vehicle. Then, the acceleration control of the vehicle is carried out by generating input signals of the ECU through a speed control unit using these analyzed APS signals. Speed control unit was designed from author of mechatronics lab.

## 2.3 Brake control system

A brake system was configured with an actuator. The brake system for implementing deceleration control of the vehicle is presented in Fig. 4. An RC servo motor is controlled by 18 steps with an operation range of  $-90^\circ \sim 90^\circ$ . Also, the servo motor is connected to the brake pedal using a steel wire and the brake pedal is pulled as the motor is started.

## 2.4 Vehicle detecting sensor

A laser scanner is used as a sensor to detect the distance between the test vehicle and a preceding vehicle for performing adaptive cruise. The laser scanner used in this research uses a TOF type that calculates the distance between two objects by measuring the travel time of a signal from the transmitter to the target and back to the receiver. The laser scanner is a LMS291-S05 by SICK, Germany, which has been widely used in developing an autonomous vehicle. The laser scanner is a divergent laser scanner with a maximum scanning angle of  $180^\circ$  and a lateral resolution of between  $0.25^\circ$  and  $1^\circ$ . Also, the laser scan is a planar scan. The elapsed time between emission and reception of the laser pulse is used to calculate the distance to the object. Fig. 5 shows the detection principle and maximum recognition range of the laser scanner.

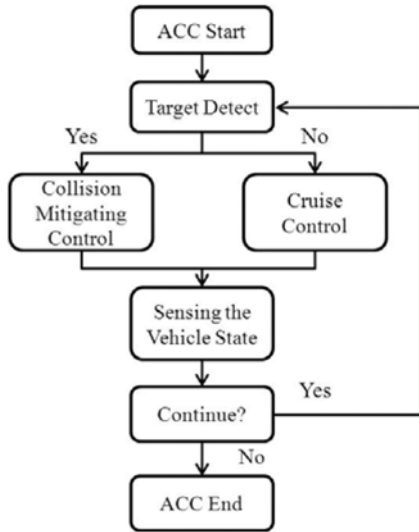


Fig. 6 A block diagram of driving algorithm

### 3. Active Cruise Control System

Basically an ACC system represents a control method that drives a vehicle by maintaining a safe distance to the preceding vehicle as it follows the preceding vehicle. In this section, a driving algorithm of the ACC system is described.

#### 3.1 Driving algorithm

The driving algorithm in an ACC system is presented in Fig. 6. The control system of the ACC system can be divided into vehicle collision mitigating control and cruise control according to the presence of a preceding vehicle. In the case of presenting a preceding vehicle, the vehicle collision mitigating control, which is based on a safety distance to the preceding vehicle, is operated. As a preceding vehicle is not presented, the cruise control is operated as the same as the general cruise control.<sup>13</sup>

#### 3.2 Target detection

The detection of a preceding vehicle in the ACC system can be performed using a laser scanner installed on a test vehicle.

The laser scanner installed on the test vehicle produces the distance information of a polar coordinate system  $(r - \theta)$ . As shown in Fig. 7, the distance information produced in a polar coordinate system is transformed into that of a Cartesian coordinate system  $(x - y)$  where  $x$ ,  $y$  are given by Eq. (1).

$$\begin{bmatrix} x \\ y \end{bmatrix} = \begin{bmatrix} r \cos \theta \\ r \sin \theta \end{bmatrix} \quad (1)$$

Regarding the vehicle detection and vehicle distance, the vehicle distance can be obtained using the angle between the start and the end point of the edge of the preceding vehicle and its average value. In addition, the data only presented in the ROI (Region of Interest) is collected as noted in Eq. (2) in order to increase the calculation rate before detecting edge areas.<sup>14,15</sup>

$$dist_{means}(t) = \begin{cases} r_i & \text{for } |x_i| < ROI \\ r_i = \max & \text{for } |x_i| > ROI \end{cases} \quad (2)$$

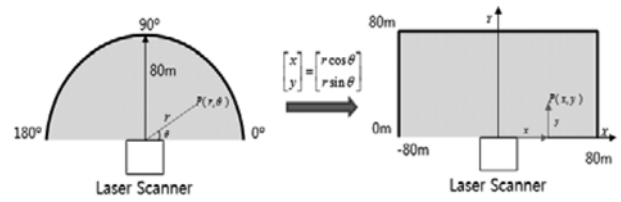


Fig. 7 Coordinate transformation of laser scan data



Fig. 8 Meaning of stop distance

where  $dist_{means}$  is the measured vehicle distance,  $i$  shows the term of  $\theta$  as the angular resolution of a sensor determined by the index of data,  $r$  is the distance between the detected point and the sensor,  $x$  is the  $x$  value in the Cartesian coordinate system transformed from its polar coordinate system, and  $\max$  represents the detectable maximum range of the laser scanner. In this study, the laser scanner's maximum range is 80 m and define the sampling time is 26 ms.

#### 3.3 Safety distance

The safety distance determined in the domestic road traffic law declares that a vehicle, which follows a preceding vehicle in the same direction, should ensure a vehicle distance to avoid a possible collision.

Thus, the safety distance that can avoid a collision with a preceding vehicle is defined by the stop distance of a succeeding vehicle according to the velocity of the succeeding vehicle.

The stop distance of a vehicle is usually determined by the sum of the thinking running distance and braking distance of the vehicle as shown in Eq. (3). Also, its configuration is presented in Fig. 8.

$$dist_{stop} = dist_{brake} + dist_{thinking} \quad (3)$$

where  $dist_{brake}$  is the braking distance and  $dist_{thinking}$  is the thinking running distance.

Therefore,  $dist_{stop}$  represents the sum of the braking distance and the thinking running distance and the safety distance to the preceding vehicle in adaptive cruise can be defined as the stop distance presented in Eq. (3).

The braking distance in a vehicle can be defined as Eq. (4) based on the Newton's second law of motion.

$$Ma_x = -\frac{W}{g}D_x = -F_{x_1} - F_{x_2} - D_A - wh \sin \theta \quad (4)$$

where  $M$  is the vehicle mass, the term of  $W = Mg$  is the acceleration of gravity of the vehicle, the term of  $D_x = -a_x$  is linear deceleration,  $D_A$  is air resistance,  $F_{x_1}$  is the front axle braking power, and  $F_{x_2}$  is the rear axle braking power generated by the brake torque. And  $h$  is center of gravity height.

The velocity of the vehicle is low speed and if the force applied to a vehicle is constant during braking, Eq. (5) can be derived using the following simple equation.

$$D_x = \frac{F_{xt}}{M} = -\frac{dV}{dt} \quad (5)$$

where  $F_{xt}$  is the force applied to the vehicle generated by longitudinal deceleration. As  $F_{xt}$  is constant, the integration from  $V_0$  to  $V_f$  is presented as Eq. (6).

$$\int_{V_0}^{V_f} dV = -\frac{F_{xt}}{M} \int_0^{t_s} dt \quad (6)$$

$$V_0 - V_f = \frac{F_{xt} t_s}{M}$$

where  $V_0$  is initial velocity in a brake application and  $V_f$  is final velocity resulting from a brake application. Thus, the running distance,  $X$ , in deceleration can be determined as an equation of velocity and distance as noted in Eq. (7).

$$\frac{V_0^2 - V_f^2}{2} = \frac{F_{xt} X}{M} \quad (7)$$

Here, because  $V_f$  becomes 0 as the vehicle is stopped due to deceleration, the braking distance caused by the deceleration can be obtained using Eq. (8).

$$dist_{brake} = \frac{V_0^2}{2 \frac{F_{xt}}{M}} = \frac{V_0^2}{2D_x} \quad (8)$$

That is, it reveals that the braking distance is proportional to the square of velocity.

In addition, the deceleration caused by air resistance during deceleration cannot be neglected. The aerodynamic drag of the vehicle is related to the aerodynamic drag coefficient and the square of velocity can be defined as Eq. (9).

$$\sum F_x = F_{brake} + CV^2 \quad (9)$$

where  $F_{brake}$  is the total braking power of the front and rear wheels and  $C$  is aerodynamic drag. Thus, the braking distance of the vehicle considering the aerodynamic drag is presented in Eq. (10).

$$dist_{brake} = \frac{M}{2C} \ln \left[ \frac{F_{brake} + CV_0^2}{F_{brake}} \right] \quad (10)$$

The thinking running distance can be obtained by the square of driver response time as a driver senses the danger of vehicle speed. However, as an automatic control system replaces a braking behavior of a driver, the thinking running distance can be determined by the sampling time of a sensor. Thus, the thinking running distance in adaptive cruise can be determined as Eq. (11).

$$dist_{thinking} = v \times Sampling\ Time \quad (11)$$

The error of the vehicle distance is determined by subtracting the distance measured by the laser scanner from the safety distance of the succeeding vehicle obtained using Eq. (3). Also, its configuration is presented in Fig. 9.

The error of the vehicle distance can be defined as Eq. (12).

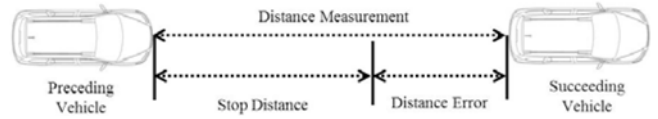


Fig. 9 Distance in ACC system.

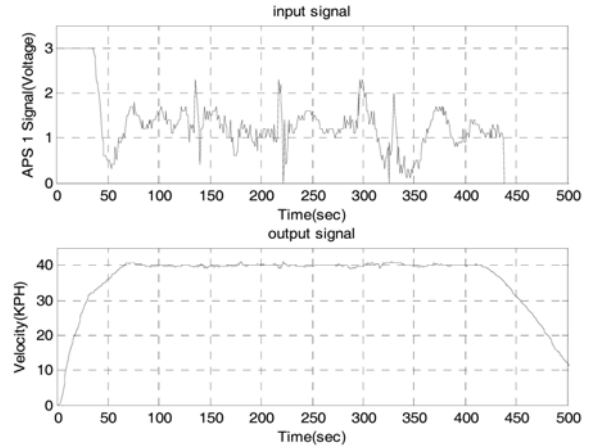


Fig. 10 Transfer function of input of output signal

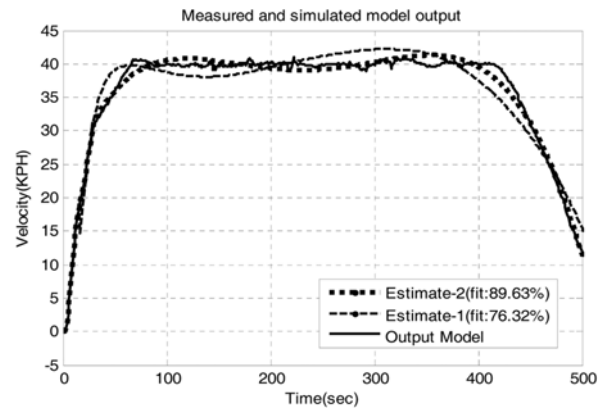


Fig. 11 Measured and simulated output

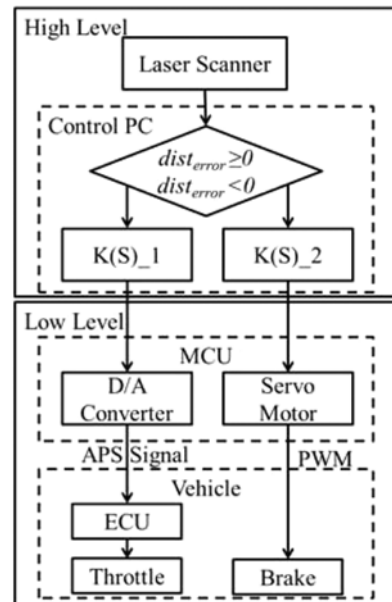


Fig. 12 ACC system configuration

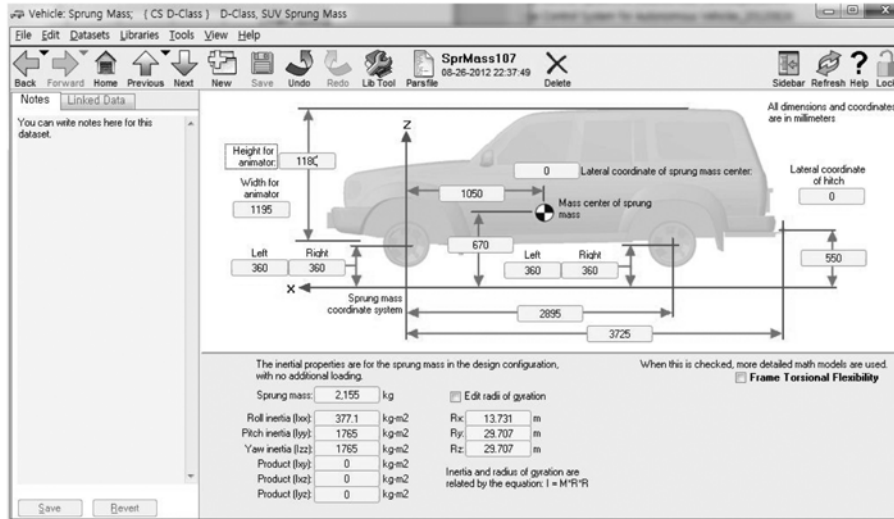


Fig. 13 Sprung mass of vehicle with CARSIM

$$dist_{error} = dist_{means} - dist_{stop} \quad (12)$$

The acceleration/deceleration controllers in adaptive cruise are designed under the condition where the succeeding vehicle maintains its safety distance to a preceding vehicle based on the error between vehicles.

#### 4. Controller Design

In this section the configuration of the accelerator and control system in a vehicle using system identification is described.

##### 4.1 System identification

A system identification method deals with the issue of finding a mathematical model of a dynamic model based on the measured data.<sup>16</sup>

In this study, the transfer function of an acceleration controller was derived using the System Identification Toolbox of MATLAB.

The input and output of the acceleration controller are determined by the voltage value of APS and the velocity, respectively. Fig. 10 shows the signals of the input and output.

The order and control coefficient of the transfer function were derived using the input and output signals of the acceleration controller. Fig. 11 represents its estimation performance.

In the case of estimate-2, it showed the results of its optimal condition as 89.63%.

Thus, the transfer function derived by applying the system identification method<sup>16</sup> can be noted in Eq. (13).

$$G(s) = e^{-2.102s} \frac{6658.31s + 5.6903}{506497.96s^3 + 325050.51s^2 + 2549.39s + 1} \quad (13)$$

##### 4.2 ACC system configuration

The control system in this research is divided into High and Low Levels and its configuration is presented in Fig. 12.

In the High Level, for  $dist_{error} \geq 0$  it represents acceleration based on the error of the vehicle distance and for  $dist_{error} < 0$  it shows

deceleration according to input velocities. The PID controller, which applies acceleration/deceleration switching logics, in Fig. 12 exhibits  $K(S)_1$  and  $K(S)_2$  and can be defined as Eq. (14) and Eq. (15).

$$\alpha(i) = Kp_a e(i) + Ki_a \int e(i) dt + Kd_a \frac{e(i) - e(i-1)}{\Delta t} \quad (14)$$

$$\beta(i) = Kp_b e(i) + Ki_b \int e(i) dt + Kd_b \frac{e(i) - e(i-1)}{\Delta t} \quad (15)$$

The term of  $\alpha$  for the acceleration in Eq. (14) is the target control position value of the acceleration pedal and the term of  $\beta$  in Eq. (15) is the angle of the control target position of the brake pedal. Also, the terms of  $Kp$ ,  $Ki$  and  $Kd$  represent the control gains of the PID controller, respectively and the tuned values obtained through a simulation are used to these terms. The error of the vehicle distance is presented as  $e$ , and the initial value of the error is defined as  $e(0) > 0$ . Then, as the control input is determined as an initial value, the vehicle is stopped.

In the Low Level, the acceleration/deceleration control can be performed using a micro control unit (MCU) based on the control target value in the High Level.

#### 5. Simulation and Experiments

In this section, the adaptive cruise control system of a vehicle is tested through a simulation and the driving performance is evaluated by applying it to a practical vehicle.

##### 5.1 ACC simulation

A simulation in adaptive cruise according to the distance error between a preceding vehicle and a succeeding vehicle is performed using vehicle kinematics programs such as CARSIM and SIMULINK.

In this simulation, the driving was configured with a single direction and the air resistance applied to the vehicle was neglected. The parameter values used in this simulation were the same as the test vehicle, Mohave by Kia Motors.

Table 2 Parameters of vehicle

| Parameter       | Value | Parameter            | Value |
|-----------------|-------|----------------------|-------|
| Length (mm)     | 4,880 | Front Tread (mm)     | 1,615 |
| Width (mm)      | 1,915 | Rear Tread (mm)      | 1,625 |
| Height (mm)     | 1,810 | Weight (Kg)          | 2,155 |
| Wheel Base (mm) | 2,895 | Friction Coefficient | 0.7   |



Fig. 14 ACC simulation with CARSIM

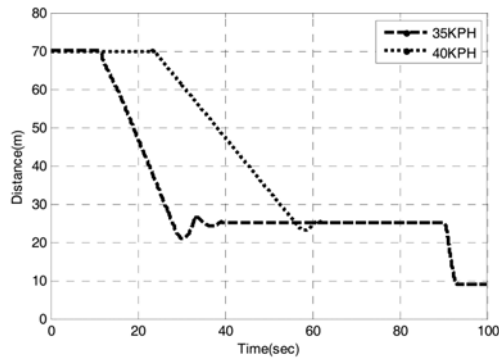


Fig. 15 Simulation results of distance tracking

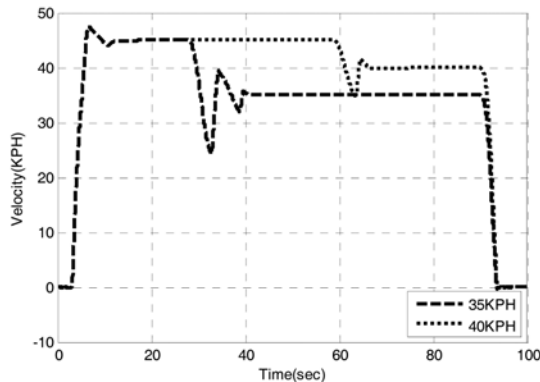


Fig. 16 Simulation results of vehicle velocity

Table 2 shows the parameter values used in this simulation. Fig. 13 represents the sprung mass of the test vehicle obtained using CARSIM.

In the simulation of ACC using CARSIM, changes in the velocity of the succeeding vehicle and vehicle distances according to the velocity of the preceding vehicle were investigated. Fig. 14 shows the results of the simulation using CARSIM. In this simulation, the initial and input velocities were 0 and 45KPH respectively. The safety distance for the input velocity of 45KPH was about 25 m calculated using the equation of the stop distance. Also, the velocities of the

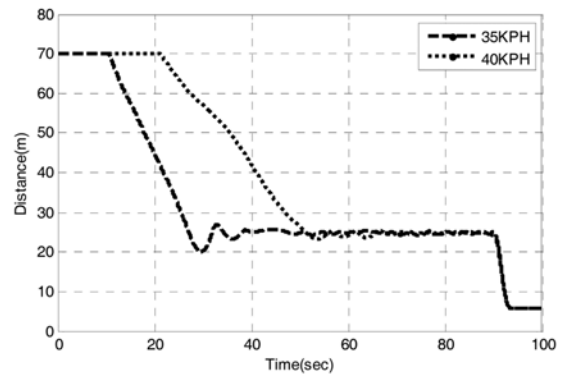


Fig. 17 Experiment results of distance tracking

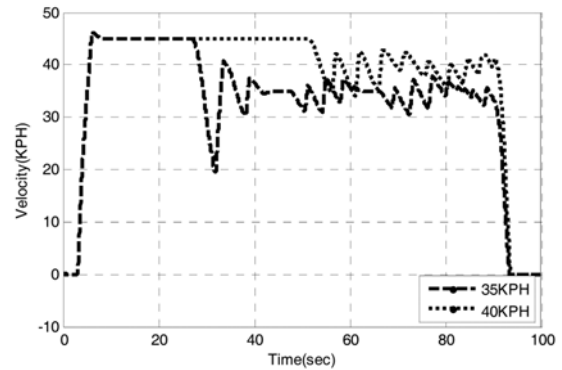


Fig. 18 Experiment results of vehicle velocity

preceding vehicle were configured by 40 and 35KPH. In addition, the initial vehicle distance between the preceding vehicle and the succeeding vehicle was configured by 70 m, which is the maximum measurement range of the laser scanner.

Fig. 15 and Fig. 16 represent the vehicle distance information and velocity between succeeding vehicles, respectively, through obtaining this simulation. The succeeding vehicle drives with a uniform velocity according to input velocities and decelerates as the vehicle distance to the preceding vehicle reached the safety distance according to the input velocities. In addition, it was verified that the succeeding vehicle represents driving while maintaining a safety distance to the preceding vehicle and the succeeding vehicle was stopped at a distance of about 9 m to the preceding vehicle.

### 5.2 ACC experiment

The experiment using a practical vehicle was performed on a straight asphalt road in Dong-myeon, Yangsan City, Gyung-sangnam-do, as the same way as its simulation.

The vehicle distance and velocity obtained using a practical vehicle are presented in Fig. 17 and Fig. 18, respectively.

The experiment performed using a practical vehicle showed similar driving characteristics to the simulation. However, errors of the vehicle distance and velocity were instantaneously occurred due to nonlinear elements of the parameters in a practical environment. In the experiment of applying practical driving, the succeeding vehicle showed uniform driving according to input velocities and maintained a safety distance to a preceding vehicle. In addition, it was verified that the test vehicle stopped with a distance of about 6 m.

Table 3 Results of simulation and experiment

| Simulation |                       | RMS  | MAX   |
|------------|-----------------------|------|-------|
| 35KPH      | Velocity (KPH)        | 34.9 | -20.2 |
|            | Distance ( <i>m</i> ) | 24.8 | -4.2  |
| 40KPH      | Velocity (KPH)        | 39.9 | -9.3  |
|            | Distance ( <i>m</i> ) | 24.9 | -1.9  |
| Experiment |                       | RMS  | MAX   |
| 35KPH      | Velocity (KPH)        | 34.5 | -21.1 |
|            | Distance ( <i>m</i> ) | 24.7 | -4.9  |
| 40KPH      | Velocity (KPH)        | 39.4 | -9.5  |
|            | Distance ( <i>m</i> ) | 24.6 | -2.4  |

### 5.3 Results

Table 3 shows the results of the driving test of the ACC system using the simulation and practical vehicle.

The average and maximum errors in this experiment obtained by the simulation and practical vehicle represented similar levels. The larger differences in the velocity of the preceding vehicle were presented in the simulation and practical vehicle test, the larger errors in the maximum velocity and vehicle distance were occurred. However, because these errors occurred at a section that decreased the velocity to maintain a safety distance to the preceding vehicle, it was considered that the errors were not a fatal level for vehicle collisions. In addition, although the velocity errors instantaneously occurred in this practical test, the average velocity error was small and the test vehicle maintained a specific safety distance according to the input velocity of the succeeding vehicle, regardless of the velocity of the preceding vehicle.

Therefore, it is considered that the driving performance of the ACC system using the longitudinal control proposed in this research showed safety driving based on the results of the experiment using a practical vehicle.

## 6. Conclusion

In this research, an ACC system that is prior to ensure safety based on the vehicle distance in autonomous vehicles was developed. A PID controller was designed to perform the longitudinal control of a vehicle. Also, a single laser scanner sensor was used to react to a preceding vehicle detected during driving and its performance was verified. By using the single laser scanner sensor, a driving algorithm that maintains and controls a safety distance to the preceding vehicle according to input velocities was proposed. Furthermore, a system that can be directly applied to general purpose vehicles using an APS system was proposed. The conventional acceleration system represented difficulties in its expansion because it applied a method that uses actuators and that showed difficulties of applying it to general purpose vehicle other than experimental vehicles.

The laser scanner sensor affects the vehicle velocity due to its detection range. Thus, in future researches, it is possible to perform more active driving through detecting long distanced vehicles or obstacles and controlling its moving directions and velocities using vision sensors.

## ACKNOWLEDGEMENT

This research was supported by the Brain Korea 21 and 2010 Autonomous Vehicle Competition (AVC) by Hyundai Motor Group of Korea.

## REFERENCES

- Lee, M. H., Lee, K. S., Park, H. G., Cha, Y. C., Kim, D. J., Kim, B., Hong, S., and Chun, H. H., "Lateral Controller Design for an Unmanned Vehicle via Kalman Filtering," *International Journal of Automotive Technology*, Vol. 13, No. 5, pp. 801-807, 2012.
- Lee, M. H., Park, W. C., Lee, K. S., Hong, S., Park, H. G., Chun, H. H., and Harashima, F., "Observability Analysis Techniques on Inertial Navigation Systems," *Journal of System Design and Dynamics*, Vol. 6, No. 1, pp. 28-44, 2012.
- Lee, M. H., Lee, H. M., Lee, K. S., Ha, S. K., Bae, J. I., Park, J. H., Park, H. G., Choi, H. J., and Chun, H. H., "Development of Hardware in the Loop Simulation System for Electric Power Steering in the Vehicle," *International Journal of Automotive Technology*, Vol. 12, No. 5, pp. 733-744, 2011.
- Shin, T. Y., Kim, S. Y., Choi, J. Y., Yoon, K. S., and Lee, M. H., "Modified Lateral Control of an Autonomous Vehicle by a Look-ahead and Look-down Sensing," *International Journal of Automotive Technology*, Vol. 12, No. 1, pp. 103-110, 2011.
- Lee, M. H., Lee, K. S., Park, H. G., Chun, H. H., and Ryu, J. H., "Robust Lateral Controller for an Unmanned Vehicle via a System Identification Method," *Journal of Mechanical Systems for Transportation and Logistics*, Vol. 3, No. 3, pp. 504-520, 2010.
- Lee, M. H., Lee, J. H., Koh, Y. H., Park, H. G., Moon, J. H., and Hong, S. P., "Observability and Estimability Analysis of the GPS and INS in the Vehicle," *Journal of Mechanical Systems for Transportation and Logistics*, Vol. 3, No. 3, pp. 537-551, 2010.
- Hong, S., Lee, M. H., Chun, H. H., Kwon, S. H., and Speyer, J. L., "Experimental Study on the Estimation of Lever Arm in GPS/INS," *IEEE Transactions on Vehicular Technology*, Vol. 55, No. 2, pp. 431-448, 2006.
- Jeong, S. H., Lee, J. E., Choi, S. U., Oh, J. N., and Lee, K. H., "Technology analysis and low-cost design of automotive radar for adaptive cruise control system," *International Journal of Automotive Technology*, Vol. 13, No. 7, pp. 1133-1140, 2012.
- Chang, T. H., Wang, M. C., and Yu, S. M., "Advance-F automatic car-following model and its traffic characteristics," *International Journal of Automotive Technology*, Vol. 12, No. 6, pp. 933-942, 2011.
- Yun, D., Kim, H., and Boo, K., "Brake performance evaluation of ABS with sliding mode controller on a split road with driver model," *Int. J. Precis. Eng. Manuf.*, Vol. 12, No. 1, pp. 31-38, 2011.
- Teguri, Y., "Laser sensor for Low-Speed Cruise Control," *SAE*

- Convergence International Congress & Exposition on Transportation Electronics, Paper No. 2004-21-0058, 2004.
12. Benalie, N., Pananurak, W., Thanok, S., and Parnichkun, M., "Improvement of Adaptive Cruise Control System based on Speed Characteristics and Time Headway," The 2009 IEEE/RSJ International Conference on Intelligent Robots and Systems, pp. 2403-2408, 2009.
  13. Venhovens, P., Naab, K., and Adiprasito, B., "Stop and Go Cruise Control," International Journal of Automotive Technology, Vol. 1, No. 2, pp. 61-69, 2000.
  14. Fayad, F. and Cherfaoui, V., "Tracking Objects Using a Laser Scanner in Driving Situation Based on Modeling Target Shape," IEEE Intelligent Vehicles Symposium, pp. 44-49, 2007.
  15. Kyriakopoulos, K. J. and Skounakis, N., "Moving Obstacle Detection for a Skid-Steered Vehicle Endowed with a Single 2-D Laser Scanner," Proceedings of the 2003 IEEE International Conference on Robotics & Automation, pp. 7-12, 2003.
  16. Lee, M. H., Park, H. G., Lee, W. B., Lee, K. S., Jeong, W. B., Yoon, K. S., Chun, H. H., and Choi, K. K., "On the Design of a Disturbance Observer for Moving Target Tracking of an Autonomous Surveillance Robot," International Journal of Control, Automation, and Systems, Vol. 10, No. 1, pp. 117-125, 2012.